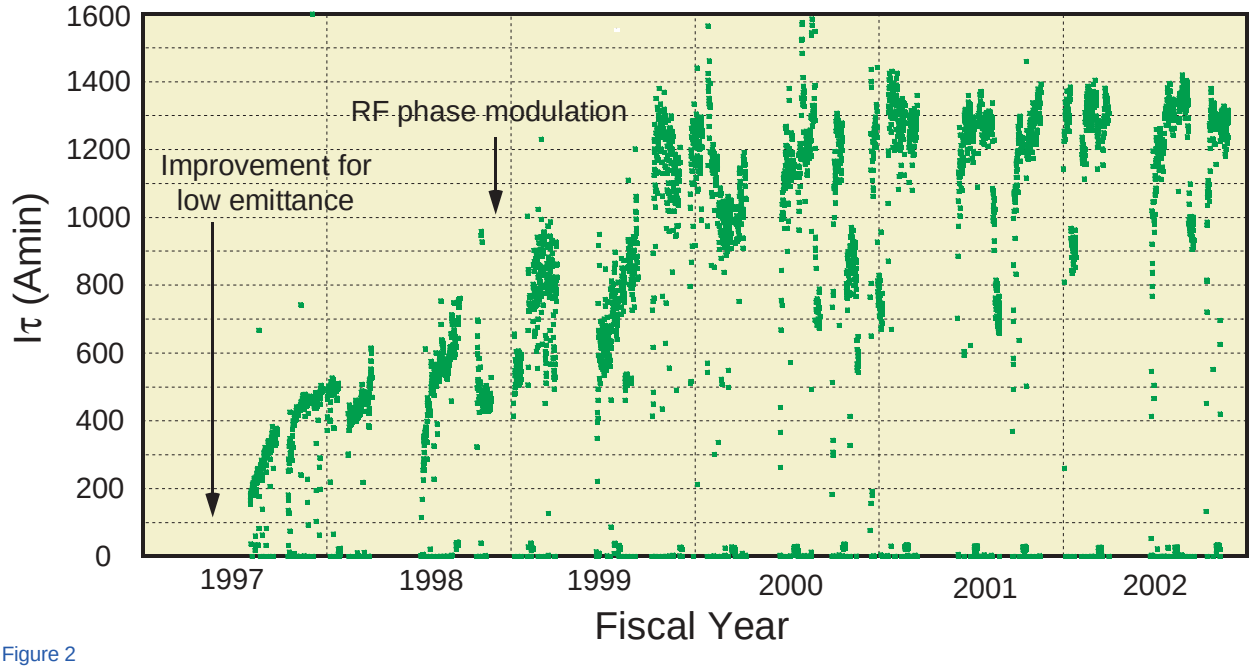

Figure 2
Iτ history of the PF Storage Ring over the past 6 years.

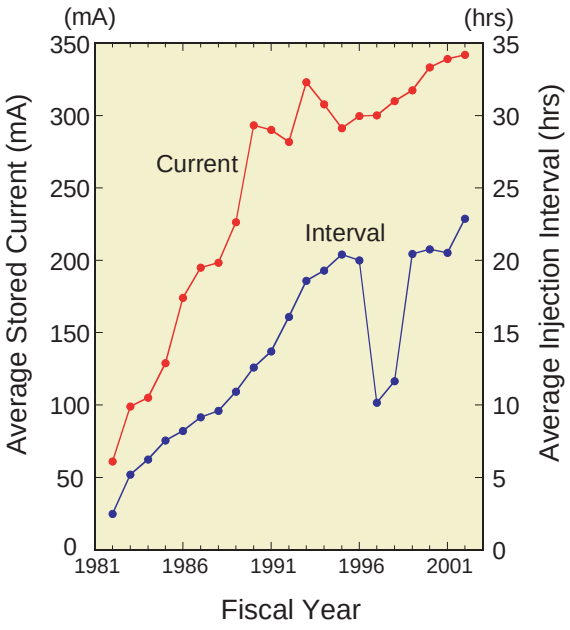

Figure 3
Average current and injection interval of the PF Storage Ring.

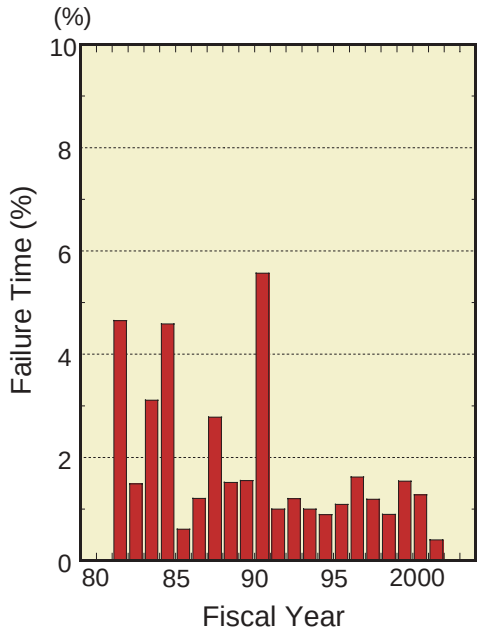

Figure 4
Failure time history of the PF Storage Ring.

2-2 The Straight-Sections Upgrade Project

Overview

In the PF ring, six insertion devices including one super-conducting wiggler are currently installed. The upgrade project [1] is a plan to double the number of straight sections available for insertion devices. As shown in Fig. 5, all quadrupole magnets around the straight sections are to be replaced with new ones having shorter lengths and higher fields in positions closer to their neighboring bending magnets. Short straight sections of 1.4 m will be created by replacing triplet magnets by pairs of doublet magnets as shown in Fig. 6. The lengths of all existing straight sections will be extended. The extension of the longest straight section is shown in Fig. 7. The PF storage ring will then have two straight sections of 9 m length, four of 5.7 m, four of 5 m and four of 1.4 m. When the upgrade alterations are completed, 11 straight sections will be available for insertion devices. In addition, two short insertion devices may be installed in the two 5.7 m-long straight sections where the RF cavities are placed. The dispersion and the betatron functions of these sections will be optimized to be as low as possible. In particular, the vertical betatron function of the short straight section will be reduced to a minimum value of 0.4

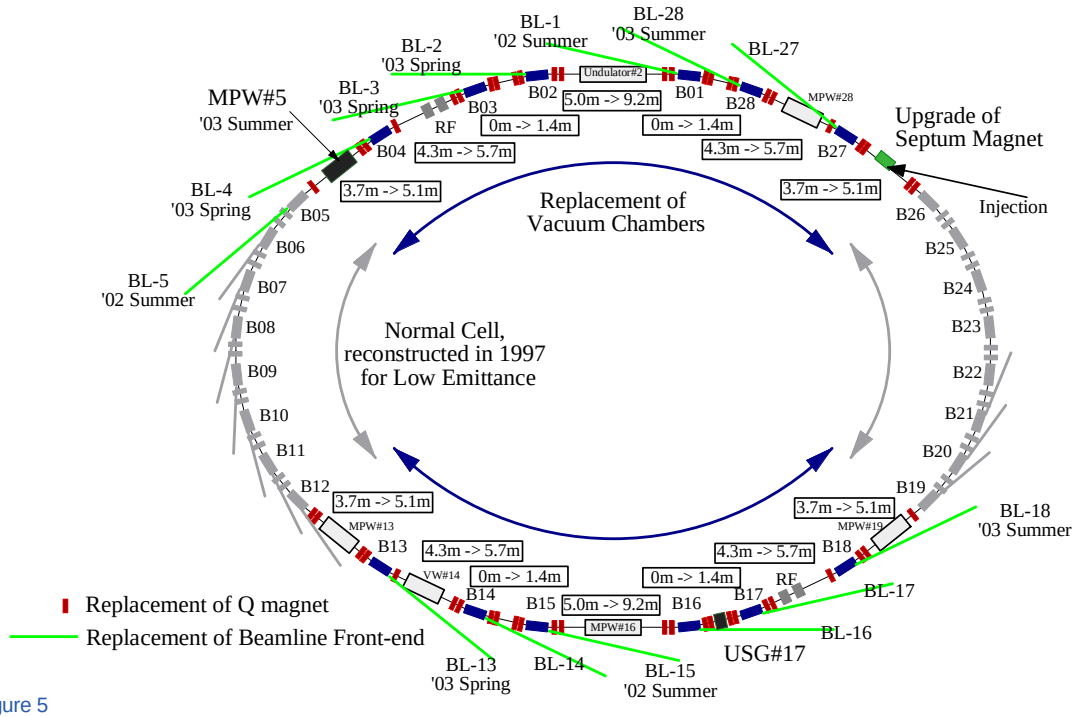

Figure 5
Outline of the upgrade project.

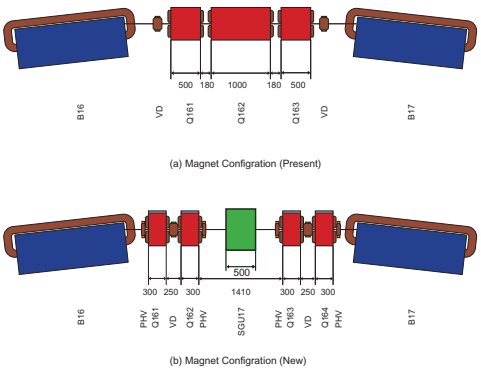

Figure 6
Creation of the short straight section.

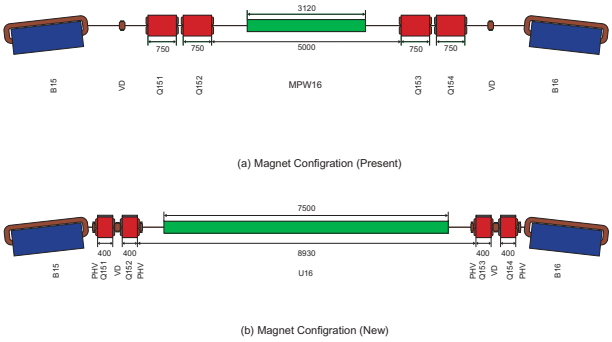

Figure 7
Extension of the longest straight section.

m. A short-period narrow-gap undulator suitable for X-ray research fields is proposed as a light source using the short straight section.

In order to modify the lattice configuration, replacement of the vacuum ducts in two thirds of the storage ring is planned. The replacement of 13 front-ends related to the straight sections will be accomplished prior to the whole reconstruction of the ring. In the autumn of 2003, a new beamline for protein crystallography will be commissioned at BL-5, the last straight section in the present configuration. Installation of a new multipole wiggler into BL-5 is scheduled for the summer shutdown of 2003. At the same time, the two straight sections of B04-B05 and B18-B19 will be partially reconstructed with new quadrupole magnets. It is expected that the whole reconstruction and re-commissioning of the ring will be completed in FY2005.

References

[1] *Photon Factory Activity Report* **2001 #19** (2003) A90.

Design of Beam Chambers

Due to new magnets and the arrangement for the upgrade of the straight sections, a number of vacuum beam chambers including those in twelve bend sections will be replaced with new ones. Some components such as RF cavities, insertion devices and beam diagnostic tools will remain. It is neccessary to maintain the same operation pressure as the present.

The cross-sectional shape of the beam channel has been decided under the following considerations.

1) It should be compatible with the new quadrupole magnet.
2) Its physical aperture must be wide enough to maintain the current vacuum beam lifetime.
3) The sensitivity of the new beam position monitor (BPM) should offer an improvement over the currently used BPM.

As a result, the beam channel becomes slim, and the sensitivity of the BPM is improved twice in the vertical direction without being degraded in the horizontal

direction. The BPM consists of four electrodes with two welded onto the top and two onto the bottom side of the beam chamber through a housing as shown in Fig. 8. The straight chamber with the BPM is installed in the quadrupole magnet and is called the Q-chamber. The total number of BPMs in the ring will be 78 including 44 new ones. The necessary number of BPM housing has already been fabricated. The main material of the beam chamber is unchanged, being aluminum alloy. The necessary amount of aluminum alloy pipes with the required cross section has been extruded to provide the material for the straight chambers.

The conceptual design of each chamber has been carried out. The pumping concept is unchanged. The main pumps used are titanium sublimation pumps, sputter ion pumps and distributed ion pumps. Much effort has been spent on the design of the bend sections. The conceptual design of the bend section is shown in Fig. 9. The B-chamber consists of a bend chamber with a synchrotron radiation (SR) port and a Q-chamber, welded through bellows. The downstream part of the SR port is exchangeable to allow for changes in the SR beamline. A pumping port is located between the bend magnet and the following quadrupole magnet as is the case currently. This is essential in order to maintain the same operation pressure. The BPM and the crotch part of the SR port are fixed points of installation and there is a bellows with RF contact at their intervals. Two-thirds of the necessary number of bellows have been prepared. Also, for precedent remodeling of the straight sections at B04-B05 and B18-B19, the necessary straight beam chambers including two Q-chambers have already been manufactured. These will be installed in FY2003.

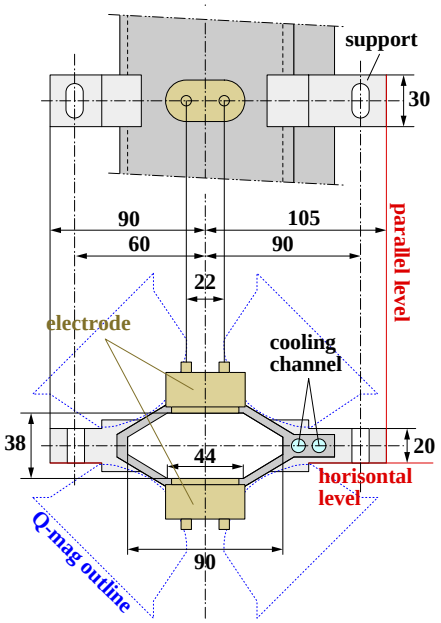

Figure 8
BPM design.

Field Measurement of the New Quadrupole Magnets

During the summer shutdown of 2003, we will replace two quadrupole magnets (Q043 and Q183) to extend the straight sections of B04-B05 and B18-B19. After the lattice rearrangement, these sections will have a longer drift space of about 1.0 m. To achieve the rearrangement, we have designed and produced new quadrupole magnets. The specification of the magnets is given in Table 2. The core length is 200 mm shorter than that of the old magnets. The correction coil is also attached for the correction of tune shifts from the insertion devices.

The field measurement was carried out using a harmonic coil to obtain the excitation curve of the field gradient and the thickness of the end-shims, which reduce the higher order multi-pole components. A photograph taken during the measurement is shown in Fig. 10, and a schematic drawing of the measurement system is shown in Fig. 11.

Table 2 Specifications of the new quadrupole magnets.

Core length	300	mm
Bore radius	35	mm
Maximum field gradient	30	T/m
Maximum current	780	A
Turn number of coil/pole	23	turns
Coil resistance at 75˚	23	mΩ
Maximum voltage	18	V

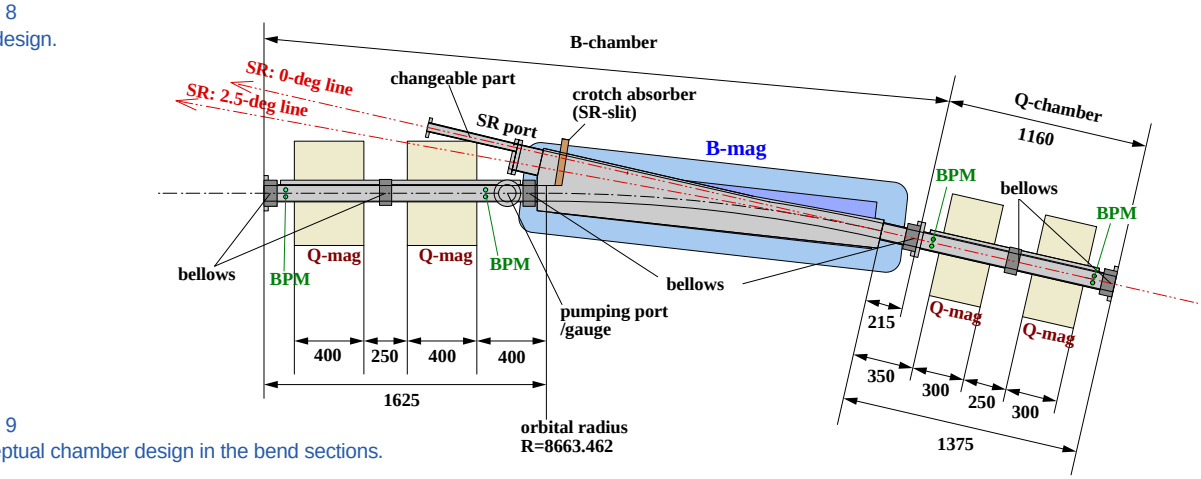

Figure 9
Conceptual chamber design in the bend sections.

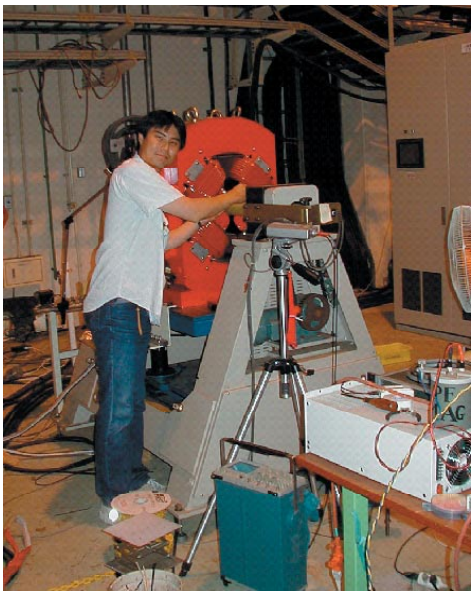

Figure 10
Photograph taken during field measurement.

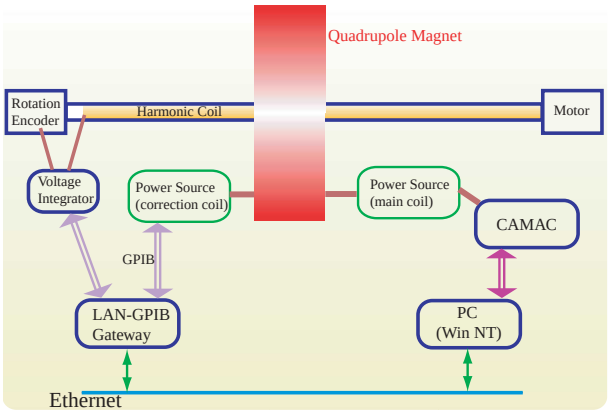

Figure 11
Schematic drawing of the measurement system.

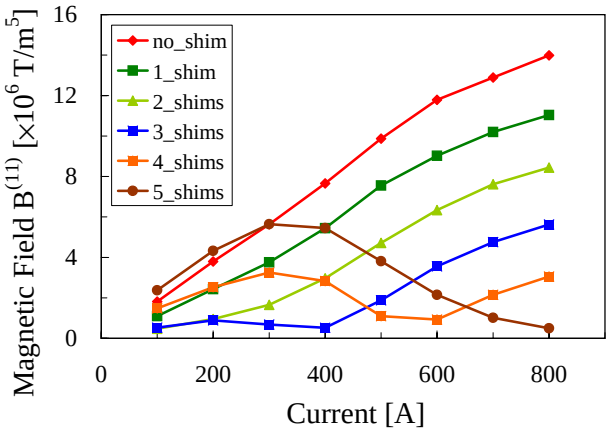

Figure 12
Dodecapole component with several end-shim thicknesses.

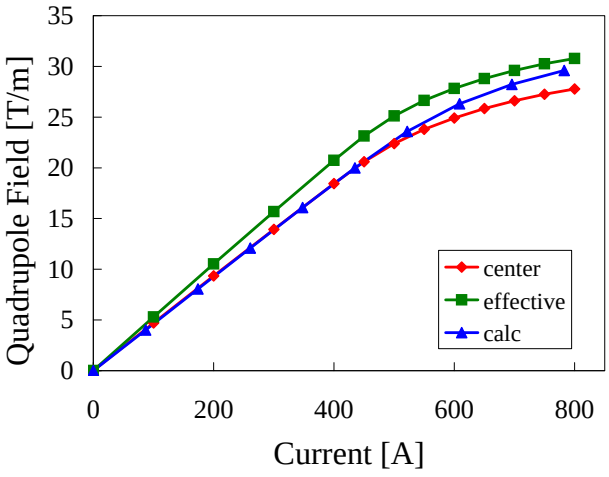

Figure 13
Excitation curves of the field gradient.

The measured results of the dodecapole component with several end-shim thicknesses are shown in Fig. 12. The field gradient of the magnets is required to be from 8.0 to 10.0 T/m in user operation, corresponding to an excitation current of 150 A to 200 A. Thus, we have selected end-shims of 4 mm thickness in order to reduce the dodecapole component as much as possible. The excitation curves of the field gradient are shown in Fig. 13. The red line shows the central field gradient measured by the short coil and the green line the effective field gradient, which is obtained by dividing the integrated field gradient by the core length. The blue line represents the results of a two-dimensional field calculation using POISSON. The measured central field gradient agrees well with the two-dimensional calculation where the field excitation is linear. We observed field saturation when the magnetic current was greater than about 500 A. In this region, the measured central field gradients are smaller than the calculation since the real magnet has a finite length. However, the effective field gradient is larger than that of the 2D calculation, and the gradient at a current of 800 A reaches 30.8 T/m. We are satisfied with the measured results for the field gradients and the strength of the higher order multi-pole components, so we will adopt quadrupole magnets of the same design in the future renewal of other straight sections.

Construction of a New Multipole Wiggler

We are constructing a new multipole wiggler (MPW#05) to be installed in the straight section between bending magnets #04 and #05. MPW#05 will be used exclusively as a light source for the beamline for protein crystallography. For this purpose, the required energy region of the synchrotron radiation is mainly 10 keV to 15 keV. In the design stage, we have tried to optimize the parameters of MPW#05 so that the photon flux density is as high as possible in this energy region, and the magnetic attractive force between the magnet arrays is minimized without a degradation of the field quality. Under the constraints of the proposed accelerator design for the present upgrade, we have found that a combination of a

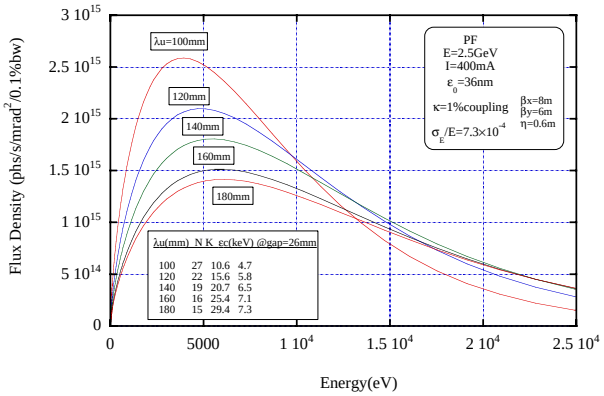

Figure 14
Comparison of the calculated photon flux densities with several period lengths. Total length of the magnet array is kept constant.

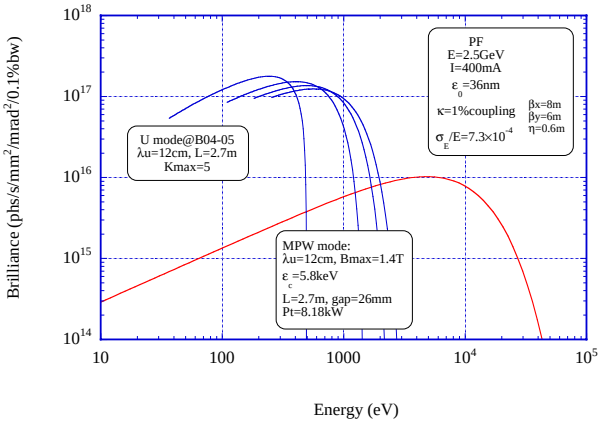

Figure 15
Spectral properties of MPW#05 in the PF ring. In addition to a wiggler mode, the spectra in the case of an undulator mode are shown.

period length of 12 cm and a periodicity of 21 is most suitable for the available length between bending magnets #04 and #05, as shown in Fig. 14.

In order to achieve the required field intensity of 1.4 T at a magnet gap of 26 mm, we adopt a hybrid magnet arrangement: NdFeB is used for the permanent magnet, and vanadium-Permendur for the iron core. The maximum K value is 15.8 at the minimum gap of 26 mm. Calculated spectra of the synchrotron radiation from MPW#05 are shown in Fig. 15: the spectra for the undulator radiation (up to the 7th harmonic) are also shown along with that for the wiggler radiation. The measurement and the adjustment of the magnetic field are performed using a 2-dimentional Hall probe system and a flipping coil system. After the field adjustment, MPW#05 will be installed in the PF ring in summer of 2003, and commissioning started in autumn.

2-3 Low Emittance Operation Study

The natural emittance of the present optics is about 36 nm·rad at 2.5 GeV and the horizontal phase advance of the normal cell about 105 degrees. We have proceeded with a machine study to search for practical operation with an increased phase advance of 125 degrees and a reduced emittance of 28 nm·rad. Figure 16 shows a comparison of the optical functions of the present optics with those of the low-emittance optics in two normal cells. As a result of the stronger focusing power necessary to increase the horizontal phase advance at the normal cell, the chromaticity becomes larger. Thus, stronger sextupole fields are required for chromatic correction, and the resultant large non-linearity reduces the dynamic aperture [1]. In fact, since the dynamic aperture was reduced by about a half compared with the present optics, beam injection became very difficult with the low-emittance optics.

In order to overcome this injection difficulty, we have designed new traveling-wave kicker magnets, which were successfully installed in October 2002. The maximum kick angle of the new kicker magnets is 3.5 mrad. The angles of the kicker and septum magnets for the low emittance optics were optimised by measuring the coherent oscillation of the injected beam by a turn-by-turn position monitor [2], and the obtained injection parameters are listed in Table 3. Since the injection rate shows a strong dependency on the betatron tune, we carried out the tune-survey around the designed tune. A tune point giving an injection rate over 1 mA/s at a repetition rate of 25 Hz was found. Figure 17 shows a typical example of the

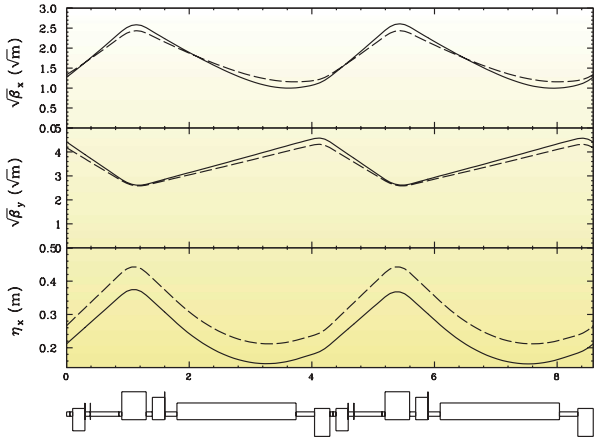

Figure 16
Optical functions of the present and the low emittance optics in two normal cells. The solid line represents the low emittance optics and the dashed line the present optics.

Table 3 Set parameter of the injection magnets. K and S indicate kicker magnets and septum magnets, respectively.

	105 deg	125 deg
K1 (mrad)	2.507	3.107
K2 (mrad)	–1.649	–2.549
K3 (mrad)	2.928	3.428
K4 (mrad)	2.912	2.812
S1 (mrad)	117.74	117.64
S2 (mrad)	101.7	102.8